NANOSTRUCTURED MATERIALS FOR SOLAR HYDROGEN PRODUCTION *

Joop SCHOONMAN[1], Roel van de KROL[2]

Sursele de energie sustenabilă ce pot fi folosite pentru a genera electroni, cum ar fi de exemplu celulele solare şi miniturbinele eoliene din mediul urban pot fi conectate la infrastructura energetică pentru a comtribui direct la reducerea emisiilor de CO_2 provenite din arderea combustibililor fosili. Utilizarea descentralizată a acestor surse de energie sustenabilă necesită sisteme de stocare. Pentru stocarea energiei electrice, sunt studiate materiale pentru acumulatoare, în special pentru baterii litiu-ion. Cu toate acestea, stocarea energiei electrice poate fi de asemenea realizată sub formă de hidrogen, ca purtător de energie. În consecinţă, au fost dezvoltate sisteme ce combină celulele solare şi electrolizoarele comerciale pentru obţinerea hidrogenului şi oxigenului din apă. O abordare mai promiţătoare este fotoelectroliza directă a apei folosind fotoanozi, materiale ce sub acţiunea părţii vizibile a radiaţiei solare pot genera oxigen, iar la contraelectrod hidrogen. Astăzi, prin diminuarea dimensiunilor la scară nanometrică a materilalelor funcţionale, producerea fotoelectrochimică a hidrogenului atrage atenţia din ce în ce mai mult. Pentru obţinerea de nanotuburi, de suprafeţe cu structură de nano-fulgi şi suprafeţe cu morfologie fractală, pentru fotoanozi o mare varietate de metode de sinteză au fost puse la punct. Optimizarea ulterioară a foto-anozilor este posibilă prin combinarea lor cu celulele fotovoltaice pentru a forma un dispozitiv monolitic în tandem. Această lucrare prezintă o trecere în revistă a materialelor avansate utilizate pentru fotoanozi, împreună cu modelele inovatoare pentru celulele fotoelectrochimice şi fotoelectrozi.

Sustainable energy sources that can be used to produce electrons, i.e., solar cells and small-scale wind turbines for the built environment, can be connected to the electricity infrastructure to directly contribute to the reduction of CO_2 emissions from fossil fuel combustion. The decentralized utilization of these sustainable energy sources requires storage. For the storage of electrical energy materials are being developed for rechargeable batteries, in particular, for lithium-ion batteries. However, storage of electrical energy can also be achieved in the form of the energy carrier hydrogen. Hereto, the combination of solar cells and commercial electrolyzers to split water into oxygen and hydrogen has been developed. A more promising development is the direct photo-electrolysis of water using photo-anode

* *The paper was presented as plenary lecture in the 17th Romanian International Conference on Chemistry and Chemical Engineering (RICCCE17), Sinaia, 2011, Romania*

[1] Prof., Department of Chemical Engineering (ChemE), Section Materials for Energy Conversion and Storage, Delft University of Technology, Julianalaan 136, 2628 BL Delft, The Netherlands, e-mail: j.schoonman@tudelft.nl, r.vandekrol@tudelft.nl

[2] Prof., Department of Chemical Engineering (ChemE), Section Materials for Energy Conversion and Storage, Delft University of Technology, Julianalaan 136, 2628 BL Delft, The Netherlands

materials, at which under irradiation of the visible part of the solar spectrum oxygen is formed and hydrogen at the counter electrode. To date, the decreasing length scale to the nano scale of the functional materials for this photo-electrochemical production of sustainable hydrogen attracts widespread attention. A variety of synthesis routes has been developed to manufacture nanotubes, nano-flake surface structures, and fractal surface morphologies for photo-anodes. Further optimization of these photo-anodes is possible by combining them with photovoltaic cells to form a monolithic tandem device. In this paper, advanced photo-anode materials will be reviewed, along with innovative photo-electrode and cell designs.

Keywords: water splitting, photo-anode, hydrogen production

1. Introduction

The industrial processes to produce the energy carrier hydrogen are based on the high-temperature steam-reforming reaction of hydrocarbons with steam and the subsequent water-gas shift reaction at lower temperatures to convert the formed CO with steam to CO_2. For methane, CH_4, the steam-reforming and water-gas shift reactions lead to four molecules of hydrogen per methane molecule. Basically, more than 90% of the yearly worldwide production of 45×10^9 kg of hydrogen is being produced using fossil fuels [1].

However, one of the principal requirements for a future Hydrogen Economy is a clean, CO_2-free, sustainable, and efficient route for the production of hydrogen, using, for example, wind and solar energy. In particular, the production of hydrogen from water and solar energy, i.e., photo-electrolysis, is one of the few methods for both renewable and sustainable energy production. Water splitting can be carried out with coupled solar cell – water electrolysis systems, and as an alternative route, the direct photo-electrolysis with a semiconductor photo-electrode, using a Photo-Electro-Chemical (PEC) cell [2].

The current generation of commercially available electrolysers has electricity-to-hydrogen conversion efficiencies of up to 85%, which seems to make this an attractive route. However, to achieve a current density of ~1 A cm^{-2} that is normally used in water electrolysers, a cell voltage of 1.9 V is required. Since the thermodynamic potential required for the splitting of water into hydrogen and oxygen is 1.23 V, the overall energy conversion efficiency has an upper limit of 65% (1.23/1.9). Hence, if the electrolyser is combined with a solar cell with a 12% conversion efficiency, the overall conversion efficiency is limited to ~8% [3]. More importantly, the cost of hydrogen produced in this manner is estimated to be ~$8/kg, well above the $2-4/kg target set by the US Department of Energy for future hydrogen production pathways [2]. In the PEC cell, the direct photo-electrolysis is a more elegant and potentially cheaper approach, because in the PEC cell the function of a solar cell and an electrolyser is combined in a single device.

In this paper the operating principles of PEC cells for the production of sustainable hydrogen will be presented. In addition, the requirements of the materials properties will be discussed briefly, along with the role of the nano dimension.

2. Photo-electrochemical production of hydrogen

In the PEC cell a photo-active semiconductor electrode and a metallic counter electrode are immersed in an aqueous solution and the photo-generated electrons and holes in the semiconductor electrode are directly used to reduce and oxidize water, respectively. Since the pioneering photo-catalysis research of Fujishima and Honda [4], who used an *n*-type rutile-structured TiO_2 photo-anode and a platinum counter electrode to split water in oxygen and hydrogen, the storage of solar energy in the form of the energy carrier hydrogen has attracted world wide attention. Their famous first demonstration of the spitting of water was performed with the electrochemical cell as presented in Fig. 1 [4].

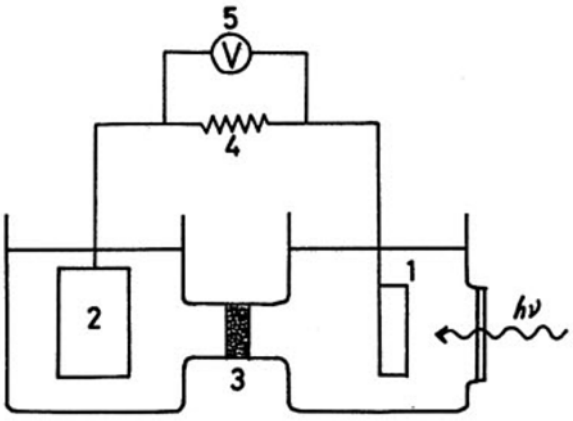

Fig. 1. Electrochemical cell in which the TiO_2 photo-electrode (1) is connected with a Pt (2) electrode in separate compartments, each with a different pH, and connected via a membrane (3). From Fujishima and Honda [4]

The operating principle of a PEC cell, comprising an *n*-type semiconducting photo-electrode and an inert metallic counter electrode immersed in an aqueous electrolyte, is illustrated in Fig. 2. The explanation of this device starts with the formation of a Schottky barrier at the interface semiconductor-aqueous electrolyte. Electrons from the n-type semiconductor will occupy surface states at the interface in order to compensate for the difference in the electrochemical potential of both phases and a space charge results in the semiconductor. When the semiconducting photo-electrode is now irradiated with

photons that have an energy equal to or beyond the bandgap of the semiconductor, electrons are photo-excited from the valence band of the semiconductor into its conduction band. Under the influence of the space charge field the photo-electrons travel to the back contact and are transported in the electrical circuit to the counter electrode, where they reduce water to form hydrogen. The photo-generated holes in the valence band of the semiconducting photo-electrode diffuse in the space-charge field to the semiconductor-electrolyte interface, where they oxidize water to form oxygen. The space-charge field prevents the recombination of the photo-excited electrons and the photo-excited electron holes.

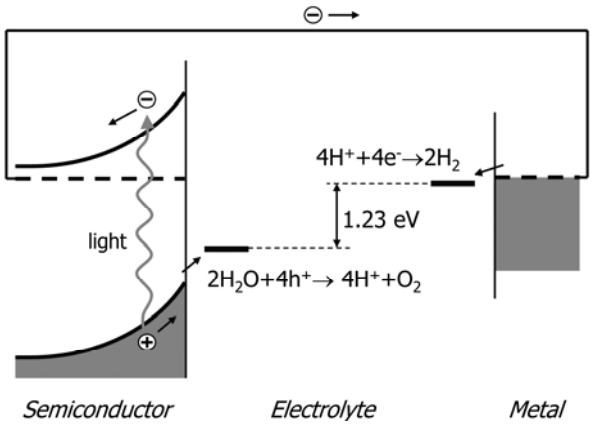

Fig. 2. Schematic energy diagram of a PEC cell with an *n*-type semiconducting photo-anode for the spitting of water in oxygen and hydrogen: The Holy Grail of Electrochemistry

3. The photo-electrode

The selection of the semiconductor electrode is of paramount importance. Suitable materials should exhibit strong visible light absorption, have a high chemical stability in the dark and under illumination, valence (E_v) and conduction (E_c) band edge positions that enable oxidation and reduction of water (see Fig. 2), efficient transport of the photo-generated electrons and electron holes in the semiconductor, low over-potentials for the electrode reactions, and low cost [5]. The bandgap of the photo-anode material determines the spectral region in which the semiconductor absorbs light. The minimum bandgap is determined by the theoretical energy required to split water (1.23 eV), plus the thermodynamic losses of about 0.4 eV [7], and the required overpotentials (~ 0.3-0.4 eV) to ensure fast electrode reaction kinetics [8,9]. Hence, the bandgap energy should be at least about 2.0 eV. At the same time, the bandgap should be small enough to ensure optimal overlap of the material's absorption with the solar spectrum (Fig. 3).

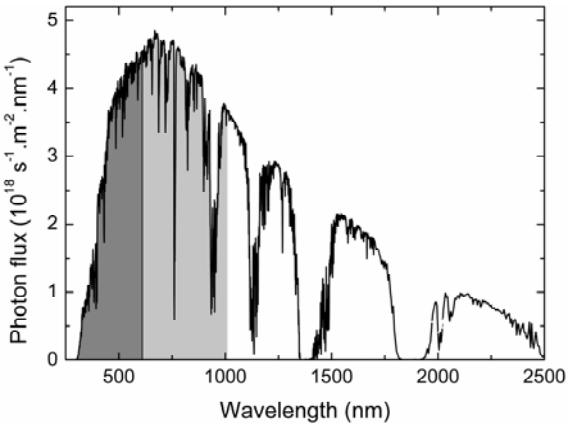

Fig. 3. The photon flux of solar radiation vs. the wavelength for AM 1.5 conditions [6]. The light-gray area corresponds to photons with an energy of at least 1.23 eV, while the dark-gray area represents the number of photons with an energy larger than 2.0 eV

4. The AM 1.5 definition

The amount of atmosphere through which radiation from the sun must pass to reach the earth's surface depends on the sun's position. This path length is usually referred to as the Air Mass (AM). The Air Mass can be expressed by the angle φ, i.e., AM=1/cos φ. When φ is 0, the sun is directly overhead and the light has to travel through 1× the thickness of the atmosphere in order to reach the earth's surface. The geometry is illustrated in Fig. 4. AM 1.5 is equivalent to a sun angle of 48.2° from overhead, and this has become the international standard of photovoltaic solar cell and PEC cell testing.

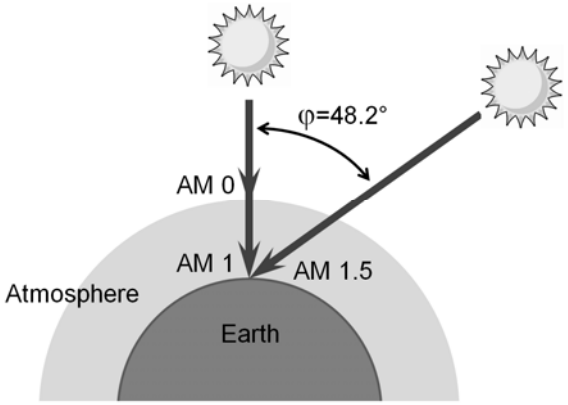

Fig. 4. Diagram that explains the relationship between the Air Mass index and the position of the sun

5. Water splitting efficiencies

The optimal bandgap energy (Eg) for photo-electrolysis can be related to the wavelength below which the material starts to absorb light (the cut-off wavelength), using Eq. (1):

$$E = \frac{hc}{\lambda} \tag{1}$$

Here, h is the Planck constant (6.626×10^{-34} J.s), c the speed of light (3×10^{8} m/s), λ is the wavelength (m) and E is the energy (J). A more convenient form of Eq. (1) reads:

$$E\ (\text{in eV}) = \frac{1240}{\lambda\ (\text{in nm})} \tag{2}$$

From the material's bandgap energy and corresponding cut-off wavelength, the maximal theoretical conversion efficiency can be calculated. This is done based on the assumption that all photons with wavelengths below the cut-off value are absorbed, and that 100% of the absorbed photons are converted to electron-hole pairs that contribute to the photocurrent, j_{photo}, and thereby also to the water splitting reaction. The expression for the so-called *applied bias photon-to-current efficiency*, or *ABPE* [10], is given by:

$$ABPE = \frac{j_{photo}\left(V_{redox} - V_{bias}\right)}{P_{light}} \tag{3}$$

Here, V_{redox} is the redox potential for water splitting (1.23 V), V_{bias} is the externally applied bias potential that is often necessary to achieve reasonable photocurrents, and P_{light} is the intensity of the incident light (~100 mW/cm^2 for AM1.5 sunlight). For a two-electrode measurement in the absence of applied bias, this expression results in the true solar-to-hydrogen conversion efficiency, η_{STH}:

$$\eta_{STH} = \frac{j_{photo}V_{redox}}{P_{light}} \tag{4}$$

Table 1

Maximum possible water splitting efficiencies for several well known semiconducting metal oxide photo-electrode materials

Material	Bandgap (eV)	η_{STH} (%)
α-Fe_2O_3	2.1	15.3
WO_3	2.5	7.5
$BiVO_4$	2.4	9.2
TaON	2.4	9.2
Cu_2O (*p*-type)	2.0	17.9
TiO_2 (anatase)	3.26	1.1
TiO_2 (rutile)	3.05	2.0

Table 1 shows the maximum achievable solar-to-hydrogen efficiencies for several widely studied photo-electrode materials calculated using Eq. (4), in which j_{photo} was determined by integrating the AM1.5 spectrum (Fig. 3) up to the cut-off wavelength.

6. Photo-anode materials - the role of doping

The traditional solar cell materials, like silicon (Si), gallium arsenide (GaAs), and cadmium telluride (CdTe) are not stable under illumination in the aqueous electrolytes of PEC cells. They either dissolve or a thin oxide film is formed which prevents electron hole transport to the semiconductor/aqueous electrolyte interface. In addition, these materials have also the disadvantage of being too expensive for use in photovoltaic solar cells (Si, GaAs), or are from an environmentally point of view not preferred (CdTe). For these reasons, the most extensively investigated class of photo-anode materials are the metal oxides. With the exception of a few cases, the general trend is that wide-bandgap metal oxide semiconductors are stable against photo-corrosion. Prime examples are the anatase and rutile polymorphs of TiO_2, α-Fe_2O_3 (hematite), and WO_3 (Table 1).

The main disadvantage of using wide-bandgap materials is the limited amount of visible light absorption. For example, TiO_2 only absorbs the near UV due to its large bandgap energy of 3.2 eV. Many research efforts have been aimed at shifting the optical absorption towards the visible part of the solar spectrum. Hereto, doping with cations and anions has been studied in detail. With regard to cation doping, the main focus has been on the transition metal ions as dopants, such as Cr and Fe [11,12]. These ions occupy Ti-sites in TiO_2 and introduce localized defect energy levels in the bandgap, as shown in Fig. 5a. Hence, excitation of electrons from these localized defect energy levels is achieved with visible light. However, the photo-generated electron holes need to hop from one energy level to another, which is a much slower process than the mobility of electron holes in the valence band. Therefore, the localized defect energy levels

increase the chance for charge trapping and recombination (Fig. 5a). In addition, dopant concentrations are small due to limited solubility and, therefore, absorption coefficients are usually very small. While some success has been achieved, the cation-doping route does not improve the over-all efficiency of photo-electrodes [5].

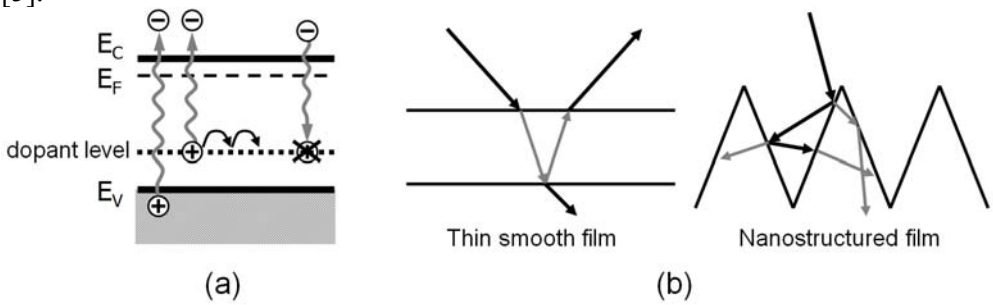

Fig. 5. (a) Diagram illustrating the use of metal 3*d* dopants to introduce localized defect levels in the bandgap of a semiconductor and enhance the visible light absorption. (b) Nanostructured morphologies increase the pathlength of the light through the material via scattering, while maintaing reasonable short pathlengths that the photo-generated have to travel in order to reach either the electrolyte or the back-contact

A decade ago, Asahi et al. reported on anion doping of TiO_2 [13]. Their quantum chemical calculations revealed that the wave functions of the anion N and C dopants show significant overlap with the oxygen valence band wave functions, which means that the sub-bandgap defect energy levels are less localized than for the cation dopants. This would reduce recombination substantially, and N and C doping of TiO_2 has indeed been shown to improved photo-catalytic activities [14-16]. The deposition of nitrogen- or carbon-doped thin film TiO_2 photo-anodes has been studied using spray pyrolysis of TiO_2 under a carbon dioxide atmosphere [17], or a high-temperature treatment in a hexane-containing environment [18]. However, the dopant concentrations were too low for a significant change in the absorption spectrum. Several routes have been studied to increase the concentration of the anion dopants N and C. The oxidative annealing of TiC films has been proposed to be a promising route [19].

7. Photo-anode materials - nanostructured surface morphologies

The ionic semiconducting metal oxides usually exhibit an indirect transition which means that the absorption of a photon is accompanied by the absorption or emission of a phonon, which is not an efficient process. It takes 0.5 to 10 μm for the incident solar radiation to be fully absorbed. In addition, the diffusion pathway of the minority carriers is usually limited. For example, the photo-excited electron holes in WO_3 and α-Fe_2O_3 recombine within 150 and less than 20 nm, respectively [20,21]. These short diffusion pathways are due to the

presence of lattice defects in these metal oxides, which can act as recombination centers. While improved thin-film synthesis techniques may lead to reduced concentrations of lattice defects, a more advanced approach is the development of nano-structured surface morphologies. As illustrated in Fig. 5b, such morphologies enhance the absorption coefficient through extensive light scattering, while the high aspect ratio ensures that the photo-generated electrons and holes have to travel only short distances to the back-contact and electrolyte, respectively.

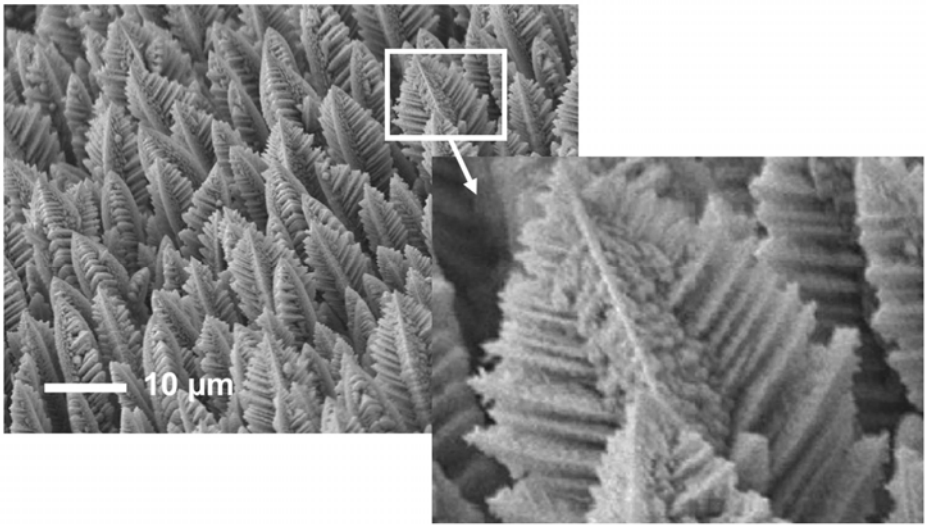

Fig. 6. Scanning electron micrograph of fractal-shaped TiO_2, co-doped with Cr and Fe, as deposited by CVD [5]

Several nano-structured surface morphologies have been reported to date. Goossens et al. [22] have described the deposition of fractal-shaped TiO_2 photo-anodes by Chemical Vapor Deposition (CVD). These undoped fractal surface morphologies do not exhibit significant photocurrents under visible-light excitation. However, Van 't Spijker et al. [23] showed that fractal-shaped TiO_2 co-doped with Fe and Cr (Fig. 6) exhibits a substantial increase in photocurrent under visible-light excitation, compared to dense undoped and dense Cr and Fe co-doped TiO_2. This shows that the nanostructured surface morphology indeed enhances the normally modest visible light absorption due to the Fe and Cr dopants. Unfortunately, extensive degradation occurs during simultaneous exposure to visible light and to water vapor or oxygen, which has been explained by the defect structure of these fractal structures.

Another approach is to make nanowire- or nanoflake-morphologies, as illustrated in Fig. 7 for Fe_2O_3 [5]. Again, the aim is to shorten the distances that the photo-generated minority carriers have to travel in order to reach the

semiconductor/electrolyte interface. The nanowire morphology in Fig. 7 was made by simply firing a piece of metallic iron foil at 800°C in air for ~6 hours. The nanoflake morphology was obtained by a similar treatment at 450°C for ~18 hours. While promising in appearance, the actual photocurrents obtained from these nanostructured electrodes are rather poor. This is attributed to the presence of sub-stoichiometric (i.e., incompletely oxidized) phases such as $Fe_{1-x}O$ and Fe_3O_4. The presence of these phases cannot be entirely avoided due to the large lattice expansion that is required for the conversion of metallic Fe to Fe_2O_3. The large interfacial stresses and strains are particularly difficult to accommodate at the interface between the Fe_2O_3 and the underlying metallic Fe substrate. While these nano-structured films are of limited use for the photo-electrolysis of water, it does illustrate that material's properties can be tuned by creating nano-structured surface morphologies.

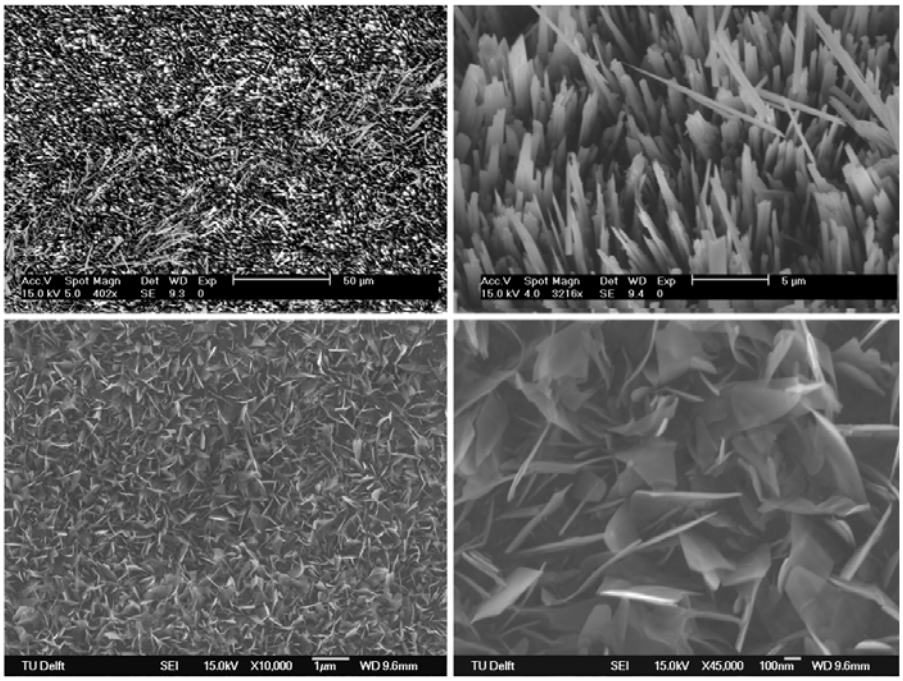

Fig. 7. Scanning electron micrograph of iron oxide nanostructures obtained by thermal oxidation of metallic iron foil in air at 800°C (nanowires, top row) and 450°C (nanoflakes, bottom row)

8. Tandem PEC devices

With bandgap values between 2.0 – 2.5 eV, materials such as Fe_2O_3 and WO_3 absorb sufficient amounts of visible light (Table 1), and do not require any dopants to enhance the optical absorption characteristics. However, there is a

trade-off involved: their relatively small bandgap results in a conduction band energy level that lies below the energy required to reduce water ($E_C < E_{red}(H_2/H^+)$). No such problem exists for the oxidation of water, oxygen evolution is energetically possible since $E_V > E_{ox}(OH^-/O_2)$.

In their seminal paper of 1972, Fujishima and Honda overcame this problem for rutile TiO_2 – which has a conduction band slightly below $E_{red}(H_2/H^+)$ – by immersing the counter electrode in a separate compartment with a different pH [4]. They essentially made use of Nernst's law to decrease $E_{red}(H_2/H^+)$ in the counter electrode compartment. However, applying such a 'chemical bias' is not a viable solution for practical devices, since the pH of both compartments will gradually become equal due to ionic transport of H^+ across the membrane (cf. Fig. 1).

A more practical solution is to apply an external bias potential to the photo-anode, which 'boosts' the energy of the photo-generated electrons to a level that allows them to reduce water. This is illustrated by Fig. 8, which shows the photocurrent as a function of applied potential for a 200 nm film of α-Fe_2O_3 doped with 0.2% Si, made by spray pyrolysis [24]. The photocurrent starts to increase at potentials positive of ~0.9 V vs. the Reversible Hydrogen Electrode (RHE). This is actually ~0.6 V more positive than one would expect, since the conduction band of α-Fe_2O_3 is ~0.3 V positive of the H_2/H^+ redox potential. One reason for this is the slow water oxidation kinetics at the Fe_2O_3 surface. This is illustrated by recent results from the Grätzel group at EPFL, who reported a 0.2 V cathodic shift of the photocurrent onset potential after applying a nanosized IrO_2 oxygen evolution co-catalyst at the surface of their nanostructured Fe_2O_3 [25]. The origin of the remaining 400 mV of additional bias required is subject to some debate, and is outside the scope of this paper.

Nearly all metal oxide photo-anodes require a bias potential, typically in the range of 0.4 – 1.2 V. When this bias is applied from an external source, it dramatically reduces the overall energy conversion efficiency, as can be seen from Eq. (3). To avoid this, one can place a photovoltaic (PV) solar cell behind the photo-anode. In such a tandem cell configuration the PV cell absorbs the low energy photons that are not absorbed by the photo-anode, and uses these to generate the required bias voltage without any efficiency penalty. PEC-PV tandem architectures have recently been explored by the EPFL group [26]. They used a dye-sensitized solar cell (DSSC) placed behind a nanostructured Fe_2O_3 photo-anode. While the concept was shown to work, efficiencies were still low due to the extensive light scattering of the Fe_2O_3 film, which prevented part of the light from reaching the DSSC.

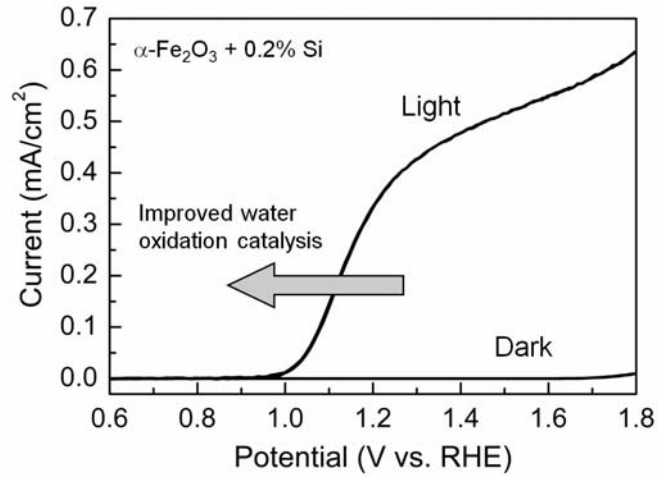

Fig. 8. Photocurrent voltammogram of a 200 nm α-Fe_2O_3 film doped with 0.2% Si illuminated with 80 mW/cm2 simulated sunlight. The voltammogram in the dark is also shown for comparison [24]

An important disadvantage of using a separate PV cell in a PEC-PV tandem architecture is that each component has to be packaged and sealed separately. This is likely to increase the fabrication costs to a level that is incompatible with the DOE's ambitious \$2-4/kg H_2 price target. To avoid this, one needs to develop monolithic tandem devices, in which the PEC and PV components are integrated within a single electrode. Already in 1998, Turner et al. demonstrated a monolithic water splitting device based on a *p*-type $GaInP_2$ photocathode biased with a GaAs *p*-*n* junction cell [27]. They reported a record solar-to-hydrogen efficiency of 12.4%, which inspired many scientists to further develop this concept and to overcome the high cost and poor stability of this particular demonstration device.

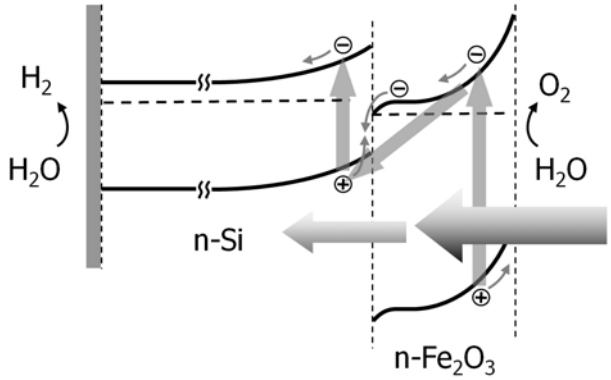

Fig. 9. Band diagram of a *n*-Si/*n*-Fe_2O_3 tandem photo-anode [1]

The tandem approach taken by our group in Delft is based on the *n-n* heterojunction device shown in Fig. 9 [1]. Wavelengths below ~600 nm are absorbed by the Fe_2O_3 photo-anode, and the photogenerated holes in Fe_2O_3 oxidize water at its surface. Higher-wavelength photons pass through the photo-anode and are absorbed by the underlying silicon. The photo-generated holes in the silicon recombine with the electrons from the Fe_2O_3, and the photo-generated electrons in the silicon have sufficient energy to reduce water. When illuminating this device with 375 nm light, all the light is absorbed within the Fe_2O_3 and no photons are able to reach the silicon. Under these conditions, the photocurrent onset potential is 1.0 V vs. RHE, comparable to the data shown in Fig. 8. When a second light source of 635 nm is now directed towards the sample, the photocurrent onset potential shows a cathodic shift of ~0.3 V due to excitation of the silicon. Although the photocurrent densities were still modest, these first experiments show that the monolithic *n-n* heterojunction tandem concept indeed works. Further improvements of the photocurrent require nanostructuring in order to address the short (~20 nm) hole diffusion length in Fe_2O_3. The device we ultimately envisage is the nanowire array tandem photo-anode shown in Fig. 10.

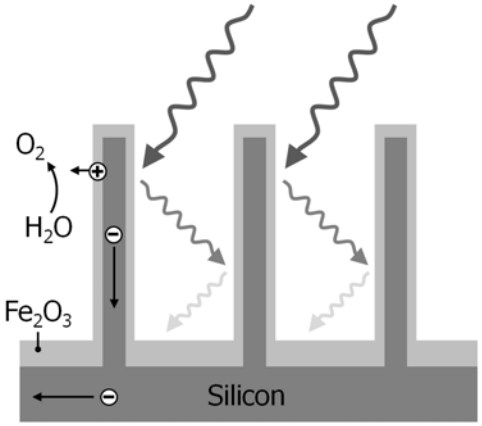

Fig. 10. Nanowire array tandem photo-anode based on a Si/Fe_2O_3 *n-n* heterojunction.

9. Conclusions

In this brief overview we have outlined the principles of direct photo-electrochemical water splitting, and listed some of the most important demands on the materials properties of photo-electrodes. Based on their stability and low cost, metal oxide semiconductors are prime candidates for this application. The main challenge is to overcome some of the intrinsic limitations that this class of materials presents: poor visible light absorption, limited charge carrier diffusion lengths, and modest catalytic activity for water oxidation. Nanostructured morphologies offer unique opportunities to address most – if not all – of these

challenges. Further progress in this exciting field requires the development of novel fabrication techniques that allows one to translate nanostructured multi-component designs into practical, low cost photo-electrodes and solar energy conversion devices.

REFERENCES

[1] *R.van de Krol, B.Dam*, Nederlands Tijdschrift voor Natuurkunde, **vol.77**, no.6, 2011, pp. 209-213 (in Dutch)

[2] *R. van de Krol, M.Grätzel (Eds)*, Photoelectrochemical Hydrogen Production. Springer 2011, (in press).

[3] *O.Khaselev, A.Bansal, J.A.Turner*, Int. J. Hydrogen Energy, **vol. 26**, 2001, pp. 127.

[4] *A.Fujishima, K.Honda*, Nature, **vol. 238**, 1972, pp. 37.

[5] *R.van de Krol, Y.Q.Liang, J.Schoonman*, J. Mater. Chem., **vol. 18**, 2008, pp. 2311.

[6] Solar irradiance data, ASTM-G173-03 (AM1.5, global tilt): http://rredc.nrel.gov/solar/spectra/am1.5/.

[7] *M.F.Weber, M.J.Dignam*, Int. J. Hydrogen Energy, **vol. 11**, 1986, pp. 225.

[8] *J.R.Bolton, S.J.Strickler, J.S.Connolly*, Nature, **vol. 316**, 1985, pp. 495.

[9] *A.B.Murphy, P.R.F.Barnes, L.K.Randeniya, I.C.Plumb, I.E.Grey, M.D.Horne, J.A.Glasscock*, Int. J. Hydrogen Energy, **vol. 31**, 2006, pp. 1999.

[10] *Z.B.Chen, T.F.Jaramillo, T.G.Deutsch, A.Kleiman-Shwarsctein, A.J.Forman, N.Gaillard, R.Garland, K.Takanabe, C.Heske, M.Sunkara, E.W.McFarland, K.Domen, E.L.Miller, J.A.Turner, H.N.Dinh*, J. Mater. Res., **vol. 25**, 2010, pp. 3.

[11] *H.P.Maruska, A.K.Ghosh*, Solar Energy Mater., **vol. 1**, 1979, pp. 237.

[12] *H.Kato, A.Kudo*, J. Phys. Chem. B, vol. 106, 2002, pp. 5029.

[13] *R.Asahi, T.Morikawa, T.Ohwaki, K.Aoki, Y.Taga*, Science, **vol. 293**, 2001, pp. 269.

[14] *S.Sakthivel, H.Kisch*, Angew. Chem. Int. Ed., **vol. 42**, 2003, pp. 4908.

[15] *S.Sakthivel, H.Kisch*, ChemPhysChem, **vol 4**, 2003, pp. 487.

[16] *X.B.Chen, Y.B.Lou, A.C.S.Samia, C.Burda, J.L.Gole*, Adv. Funct. Mater., vol 15, 2005, pp. 41.

[17] *C.S. Enache, J.Schoonman, R.van de Krol*, J. Electroceram., **vol. 13**, 2004, pp. 177.

[18] *C.S.Enache, J.Schoonman, R.van de Krol*, Appl. Surf. Sci., **vol 252**, 2006, pp. 6342.

[19] *H.Irie, Y.Watanabe, K.Hashimoto*, Chem. Lett., **vol. 32**, 2003, pp. 772.

[20] *S.J.Hong, H.Jun, P.H.Borse, J.S.Lee*, Int. J. Hydrogen Energy, **vol. 34**, 2009, pp. 3234.

[21] *A.Kay, I.Cesar, M.Grätzel*, J. Am. Chem. Soc., **vol. 128**, 2006, pp. 15714.

[22] *A.Goossens, E.L.Maloney, J.Schoonman*, Chem. Vapor Depos., **vol. 4**, 1998, pp. 109.

[23] "Unusually high photocurrents in anatase TiO_2 thin films with fractal morphologies", presented at the 16th International Conference on Photochemical Conversion and Storage of Solar Energy (IPS-16), Uppsala, Sweden, 2006

[24] *Y.Q.Liang, C.S.Enache, R.van de Krol*, Int. J. Photoenergy doi:10.1155/ 2008/739864, 2008

[25] *S.D.Tilley, M.Cornuz, K.Sivula, M.Gratzel*, Angew. Chem. Int. Ed., **vol 49**, 2010, pp. 6405.

[26] *J.Brillet, M.Cornuz, F.Le Formal, J.H.Yum, M.Grätzel, K.Sivula*, J. Mater. Res., **vol. 25**, 2010, pp. 17.

[27] *O.Khaselev, J.A.Turner*, Science, **vol. 280**, 1998, pp. 425.